Reviewer #2:

First of all, sincerely thank you very much for your valuable comments. All your suggestions are very important and have important guiding significance for our writing and research. When revising the article, we considered thoughtfully what you have advised.

1. Comment: The authors present an improvement to the multi-grid hydrological/hydrodynamic SWMM/IM-DBCM model which partitions the model domain into a coarse resolution part (away from rivers) and a fine resolution part (areas susceptible to inundation). The authors present the mesh-generation approach and test the model in 4 configurations with a variable number of grid cells (ranging between 59k-207k cells). Results of discharge are compared to observed values, inundation depth is presented without comparison to observations. Advances are said to stem from improved computational efficiency, the main reason for the multi-grid approach of the model, while retaining an acceptable model performance.

Response to comment: Thank you very much for your valuable comments. SWMM is a direct one-way coupling of semi-distributed hydrological and 1D hydrodynamic models. Since the 1D nonlinear reservoir method is used to simulate the runoff routine, it is difficult to directly coupled with 2D hydrodynamic model. The M-DBCM proposed by our team is the direct dynamic two-way coupling of distributed hydrological and 2D hydrodynamic model.

In the section 3.2, flood process in natural watershed was simulated using the improved M-DBCM. The simulation data was collected from the references, Yu and Duan (2012); Sánchez (2002); Blackmarr (1995). Only the discharge hydrographs were obtained in the observation stations, therefore, we have compared the simulated discharge hydrographs with the measured data to evaluate the performance of the proposed model.

In the proposed model, the inundation and non-inundation regions were changed with the water depth; the hydrologic and hydrodynamic models were coupled through the moving interfaces. Therefore, we have presented the water depth and positions of coupling interfaces in Figure 12 to show the changing process of inundation and non-inundation regions with water depth.

However, our current research work lacks data, especially the measured data used to evaluate the performance of proposed model. In future works, we will collect more data, such as the water depth and discharge to further evaluate the performance of proposed model.

Ref:

[1] Yu C. and Duan J. G., Simulation of Surface Runoff Using Hydrodynamic Model, Journal of Hydrologic Engineering (ASCE), 2017, 22(6): 04017006

[2] Sánchez, R. R., GIS-based upland erosion modeling, geovisualization and grid size effects on erosion simulations with CASC2DSED. Thesis (Ph. D.) --Colorado State University, 2002.
[3] Blackmarr, W., Documentation of hydrologic, geomorphic, and sediment transport measurements on the Goodwin Creek experimental watershed, northern Mississippi, for the period 1982–1993, Res. Rep. 3, Agricultural Research Service, U.S. Dept. of Agriculture, Oxford, MS, 1995.

2. Comment: The state-of-the-art approach to the problem of variable resolution grids is a coarse-resolution hydrological model coupled with a 1D river routing model that activates a 2D model when channel capacity is exceeded. While the authors acknowledge this in the manuscript, they fail to compare their approach to results of such a model chain to demonstrate their advance. Admittedly, producing the same results with such a model chain to use as a baseline is a non-trivial task, but some comparison if not in the same catchment, should be considered mandatory.

Response to comment: Thank you for reading this article carefully and making valuable suggestions. The coupling model can be divided into two types: external (one-way) and internal (two-way) coupling models (see Figure 1). And the internal coupling model can be further divided into four types, as shown in Figure 2.

The coupling of the Mike SHE and Mike11 is a typical example of the coupling of hydrologic and 1D hydrodynamic models, as shown in Figure 2(a). The application of 1D modeling of overland flow is limited when developing precise and reliable flood maps in 2D inundation regions.

To overcome the lack of 2D hydrodynamic simulation in type-1, the coupling of hydrologic, 1D, and 2D hydrodynamic models is proposed. In this coupling type, the runoff flows into the 1D river or pipes first, and the hydrologic model is coupled with the 1D hydrodynamic model. And then, the water in 1D rivers or pipes can overflow into low-lying areas, the 1D and 2D hydrodynamic models are coupled in a two-way manner. This coupling type is an indirect coupling of hydrologic and 2D hydrodynamic models, as shown in Figure 2(b). For instance, Mike SHE and Mike11 are coupled to form Mike Urban, and Mike11 and Mike21 are dynamically coupled to form Mike Flood. The indirect coupling between the hydrologic and 2D hydrodynamic models can be developed by coupling Mike Urban and Mike Flood. The 1D hydrodynamic model is a connection channel between the hydrologic and the 2D hydrodynamic models.

In the Type-3, both the overland flow migration and inundation processes are all calculated by 2D hydrodynamic model, and the runoff generation is considered as the source term of the continuity equation of 2D hydrodynamic model. The type-3 has high numerical accuracy but low computational efficiency.

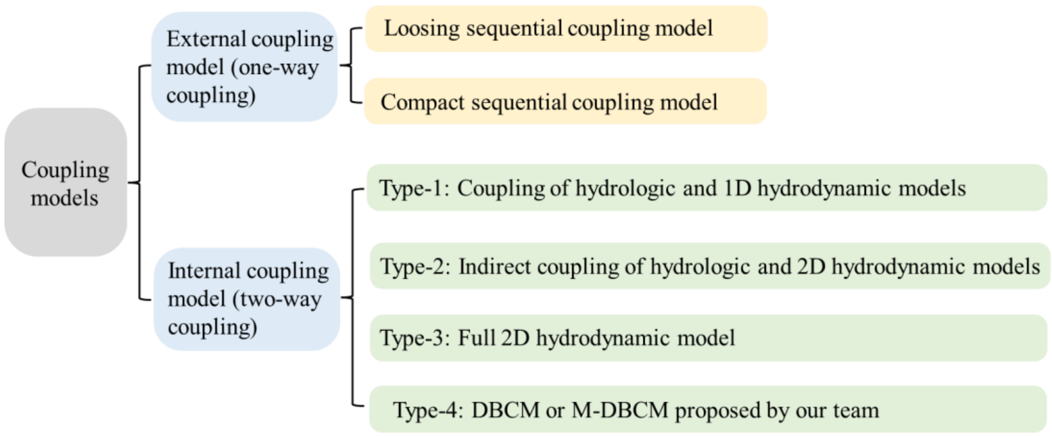

Figure 1 Classifications of coupled hydrologic and hydrodynamic models

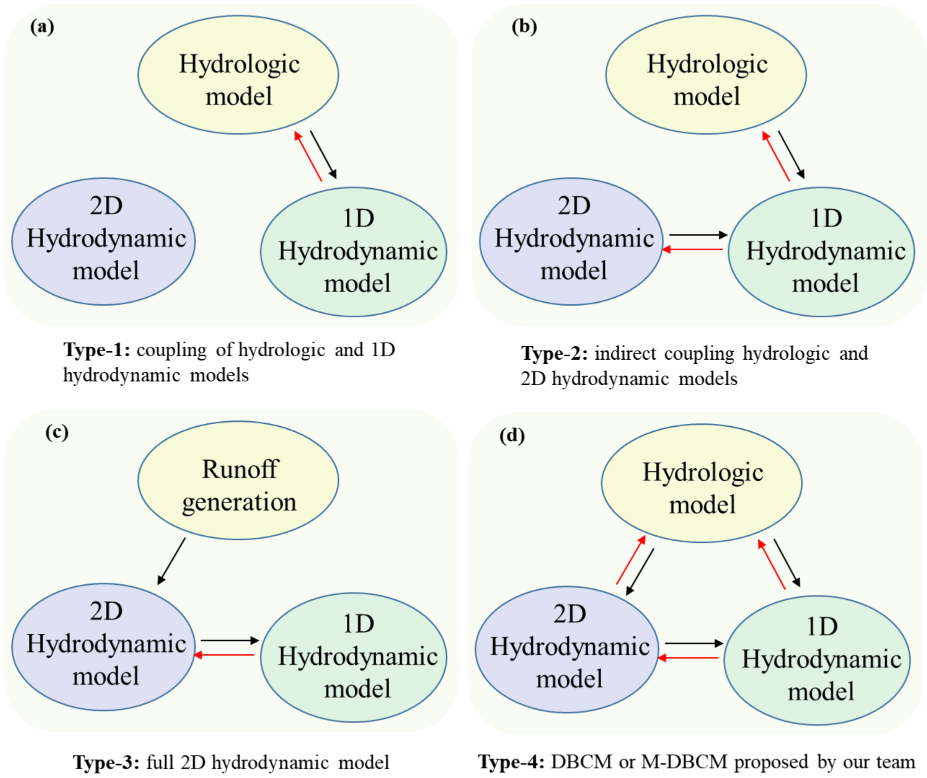

Figure 2 Classifications of internal coupling models

It is observed that existing coupling models can not realize the dynamic two-way coupling of hydrology and 2D hydrodynamic models. The 1D hydrodynamic model was used to link the hydrologic and 2D hydrodynamic models. The runoff flows into the 1D river or pipes first, and the hydrologic model is coupled with the 1D hydrodynamic model. And then, the water in 1D rivers or pipes can overflow into low-lying areas; conversely, the water in low-lying areas can flow to 1D regions in return. The 1D and 2D hydrodynamic models are coupled in a two-way manner. This coupling type is an indirect coupling of hydrologic and 2D hydrodynamic models. In reality, however, water may be discharged into both 1D channel and 2D waterbodies simultaneously, and the hydrologic, 1D, and 2D hydrodynamic models should be linked directly. Direct coupling of hydrologic and 2D hydrodynamic models can reflect the flood processes more truly, which deserves more attention.

Aiming to this problem, we have proposed a coupled hydrologic and 2D hydrodynamic models. In the proposed model, the 1D river channel and 2D inundation regions were not distinguished, and the 2D hydrodynamic model was applied to both regions.

There have been many published papers about the coupled 1D and 2D hydrodynamic models, and our future works may focus on the adding a 1D hydrodynamic model to the proposed M-DBCM, where the hydrologic model is used to simulate the runoff routing, the 1D hydrodynamic model is used to simulate the flood process in rivers and the 2D hydrodynamic model is used to reflect the inundation process in the low-lying inundation regions. Three coupling strategies, i.e., the coupled hydrologic-1D hydrodynamic module, coupled 1D-2D hydrodynamic module and coupled hydrologic-2D hydrodynamic module, are proposed.

However, the direct dynamic bidirectional coupling of distributed hydrologic and 2D hydrodynamic models is the key and important technology to develop the flood simulation models, and it is also the innovation of the M-DBCM. Besides, the multi-grids are used to divide the watershed, and the model can improve computational efficiency while maintaining numerical accuracy, which is the main difference between the proposed model and other existing models.

3. Comment: The authors present model runtimes of the four grid configurations in Fig 13. It is apparent that runtimes scale linearly when comparing the uniform grid case to the variable-grid case (cf case00 to case12). This relationship does not hold, however, in coarser configurations of the multi-grid models (cases 15/10), i.e., the runtime/grid is significantly higher. e.g., going from 105k cells to 59k cells only brings moderate efficiency savings of 10-15%. This shows the limits of the approach, presumably because more time is spent on coupling the coarse and fine grids.

Response to comment: Thank you for your valuable suggestions. We have proposed a parameter to quantitatively evaluate the computational efficiency of the M-DBCM (Shen and Jiang, 2023, http://doi.org/10.2166/hydro.2023.131). We defined the evaluation parameter as the ratio of the simulation time of the M-DBCM to that of the full 2D hydrodynamic model (HM2D), as shown in Eq. (1):

$$C = \frac{(1+\alpha_0)t_1 + t_2}{t_0} = \frac{(1+\alpha_0)\alpha \dfrac{A_1}{\Delta x_1^2}\left(\dfrac{T_{end}}{\Delta t_1}\right) + \beta \dfrac{A - A_1}{\Delta x_2^2}\left(\dfrac{T_{end}}{\Delta t_2}\right)}{\alpha \dfrac{A}{\Delta x_1^2}\left(\dfrac{T_{end}}{\Delta t_1}\right)} \tag{1}$$

where C is the assessment parameter to evaluate computational efficiency of M-DBCM;

t_1, t_2 are the computation time on fine and coarse grids, respectively (s); t_0 is the computation time of HM2D (s); Δx_1, Δx_2 are the size of fine and coarse grids (m); Δt_1, Δt_2 are the time step on fine and coarse girds (s); A_1, A_2 are the area of coarse and fine grids, respectively; T_{end} is simulation time (s); α and β are the runtime of hydrodynamic and hydrologic models at one calculation node (s), which is depended on computer power and numerical model complexity. Since the hydrodynamic model is expressed by nonlinear hyperbolic equation and hydrologic model is expressed by linear equation, the calculation of the hydrodynamic model is more complicated than that of the hydrologic model, which results $\frac{\beta}{\alpha} < 1$.

The time step ratio of coarse grids to fine grids is equal to the size ratio of coarse grids to fine grids, as follows:

$$\frac{\Delta t_2}{\Delta t_1} = \frac{\Delta x_2}{\Delta x_1} \tag{2}$$

Based on Eq. (2), Eq. (1) can be rewritten as:

$$C = \frac{A_1}{A} + \frac{\beta}{\alpha}\left(\frac{\Delta x_1}{\Delta x_2}\right)^3 \frac{A - A_1}{A} \tag{3}$$

Define $n = \frac{A_2}{A}$ ($0 < n \le 1$), $\Delta t_2 = k \Delta t_1$ ($k \ge 1$), Eq. (3) becomes

$$C = (1-n) + \frac{\beta}{\alpha}\frac{1}{k^3} n \tag{4}$$

From Eq. (4), the computational efficiency of M-DBCM is not only related to the size ratio of coarse to fine grids, but the area ratio of coarse grids to entire domain. If the area of coarse-grid regions are much greater than that of the fine-grid regions, that is, $n \to 1$, the assessment parameter becomes $C \propto \frac{\beta}{\alpha}\frac{1}{k^3}$. It is indicated that the computational efficiency of M-DBCM exponentially improves with the increasing of the size ratio, as shown in Figure 3(a). If the size of coarse grids is much more than that of fine grids, that is, $k \to \infty$, the assessment parameter becomes $C \propto (1-n)$. It is stated that the computational efficiency of M-DBCM improves linearly with the increasing of the area ratio of the coarse grids to entire domain, as shown in Figure 3(b).

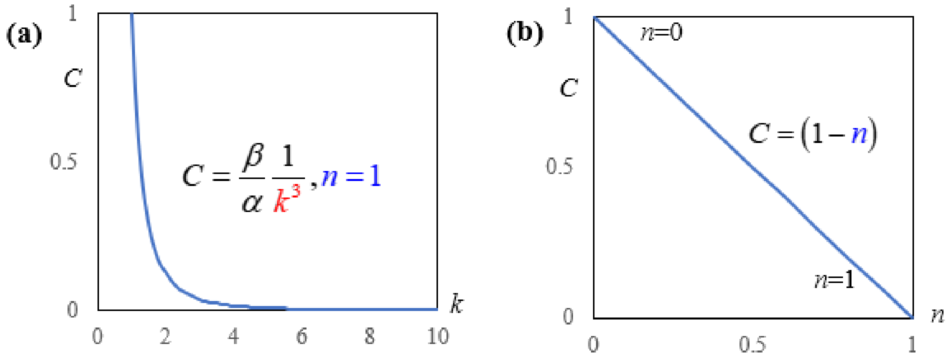

Figure 3 The relationship between the evaluation parameter and the *n* and *k*:(a) the relationship between the evaluation parameter and *n*; (b) the relationship between the evaluation parameter and *k*

We compared the graphs of three functions: $y = 1/x$, $y = 1/x^2$, $y = 1/x^3$, as shown in Figure 4. From this figure, compared with $y = 1/x$, in the $y = 1/x^3$, the *y* values decrease sharply as *x* increases. It is indicated that the computational efficiency of M-DBCM exponentially improves with the increasing of the size ratio. From this figure, in the $y = 1/x^3$, when *x*< 10, *y* values are highly variable; however, when *x*> 10, although the *y* value is decreasing, it is decreasing slowly. It is indicated that a ratio of coarse to fine grid between 1 and 10 may be suitable. We came to this conclusion after carefully reading the reviewers' comments. Thank you again for your valuable comments!

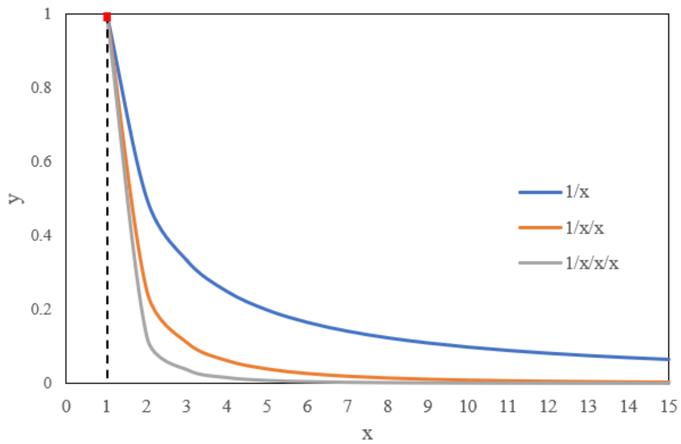

Figure 4 The graphs of $y = 1/x$, $y = 1/x^2$, $y = 1/x^3$

In the original manuscript, different cases were used to divide the Goodwin watershed, as shown in Figure 5. In the case12, case15 and case10, the number of coarse and fine grids are shown in Table 1. The number of fine grids accounts for half of the total number of grids in case12, while the number of fine grids is much greater than the number of coarse grids in case15 and case10. The calculation time of coarse and fine grids is also reported in Table 1. The size of fine grids is the same in all the cases. In case12, the size of coarse grid is twice that of the fine grid, while the size of the coarse grid is five times and ten times that of the fine grids in case15 and case10, respectively. The number of grid cells ranked from more to less is as follows: case12> case15> case10. It is well-known that the more grids mean longer computational time. Therefore, case12 cost more computation time compared with case15 and case10.

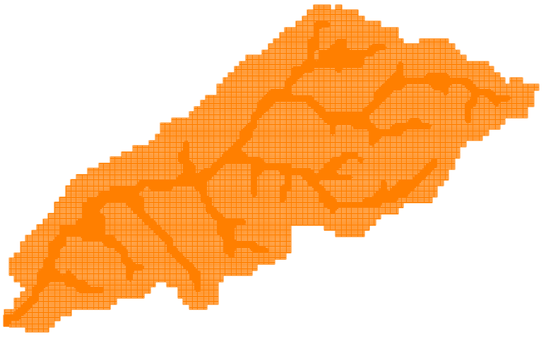

(a) case12

(b) case15

(c) case 10

Figure 5 Grid partition of different cases

Table 1 The computation time of grids with different sizes (s)

	Case12	Case15	Case10
The number of fine grids	42474	42474	42474
The number of coarse grids	42517	7425	2153
Computation time for fine grids	4910.1	4890.32	4761.88
Computation time for coarse grids	243.8	16.28	2.19
Total runtimes	6900	6206	5800

The runtimes of different cases are shown in Figure 6. The total execution time includes the time for coarse and fine grids and others, such as the input and output of data, coarse and fine grids interpolation, coupling of the hydrological and 2D hydrodynamic models, wet and dry grid judgment, and so on. It is observed that the runtime for coarse grids decreases rapidly in different cases, which is related to the number of the coarse grids. In case12, case15 and case10, the number of the coarse grids is 42517, 7425, and 2153, respectively. Therefore, the runtime for the coarse grids decreased rapidly.

However, the number of fine grids is much greater than that of the coarse grids, especially in case15 and case10. The 2D hydrodynamic model was solved in the fine-grid regions. Therefore, it cost more computational time compared with coarse grids, as shown in Figure 6, where the bule bar is the time spent on coarse grids. In all the cases, due to the large amount of calculations involved in fine grids, the time spent on fine grids accounts for a significant proportion of the total execution time. Therefore, the total computational time of all cases does not differ significantly.

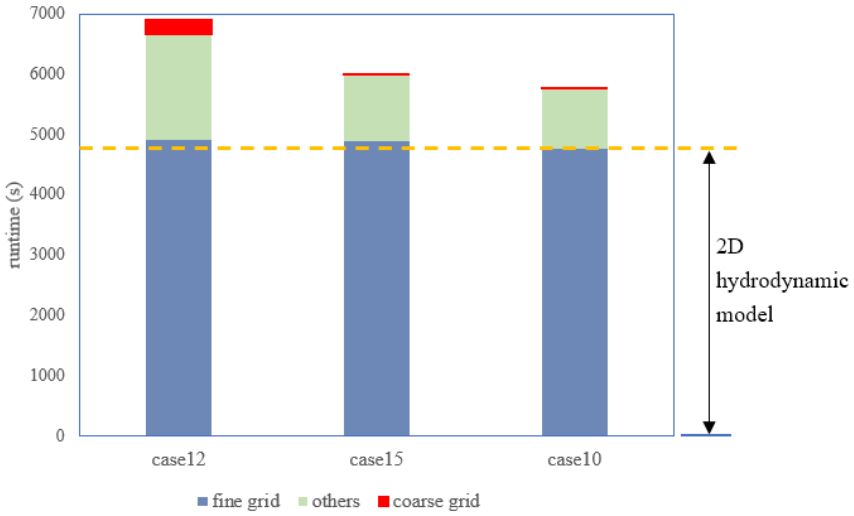

Figure 6 The runtime for coarse and fine grids and the total runtime

Besides, we have calculated an example to further evaluate the computational efficiency of the proposed model. In this example, the sketch of the case is shown in Figure 7. The length of the plane is 182.88 m. A Manning's coefficient of 0.025 s/m$^{1/3}$ is recommended. The bed slope is 0.016. The constant rainfall intensity is 50.8 mm/h. The rainfall duration is 1,800s and the total simulation time is performed for 3,600 s. Different cases with various grid size ratios were designed to evaluate the performance of the M-DBCM, as listed in Figure 8. In M-DBCM, the size of fine grids is 1.83 m while the rest of the domain is coarsened to levels higher.

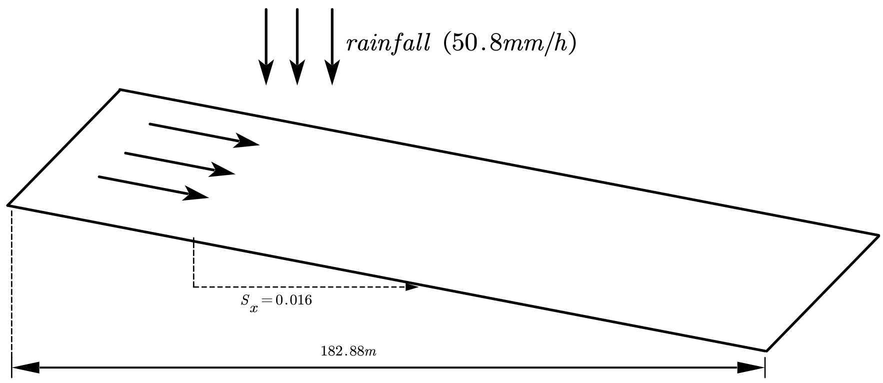

Figure 7 The schematic description of the example

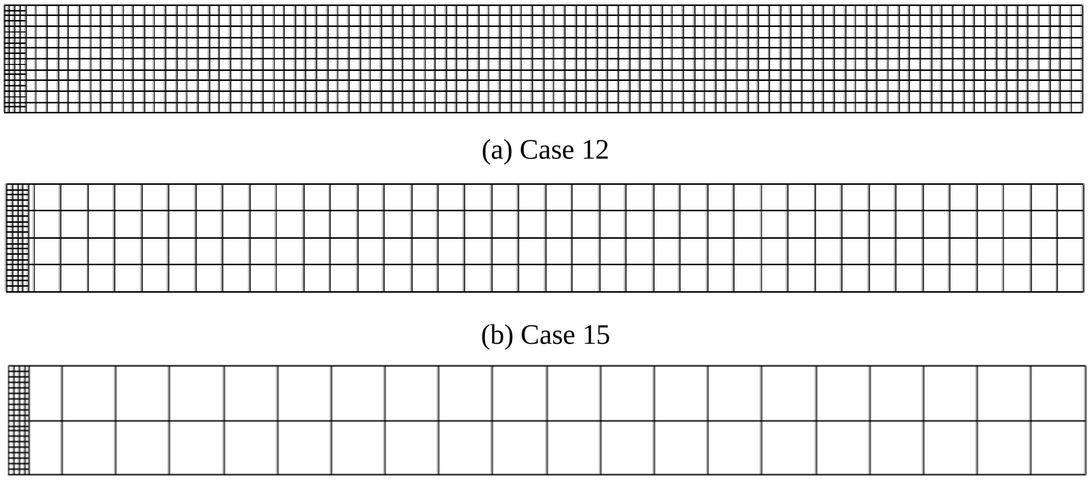

(a) Case 12

(b) Case 15

(c) Case 10

Figure 8 The different size ratios of coarse grids to fine grids

The total execution time of different cases is shown in Figure 9. It is observed that the computational time of the case15 and case10 has been significantly decreased compared with that of case12. In this example, the number of fine grids is less than that of coarse grids, as listed in Table 2. A large proportion of the time spent on coarse grids, especially in case12. With the increasing of the ratios of the coarse to fine grids, the number of coarse grids is significantly reduced. Therefore, the runtime for coarse grids decreased rapidly, and the total execution time decreased significantly. Compared with the Goodwin watershed, the fine grid regions occupy a small proportion in this example. Therefore, the total execution time decreased rapidly with the increased of the ratio of coarse to fine grids.

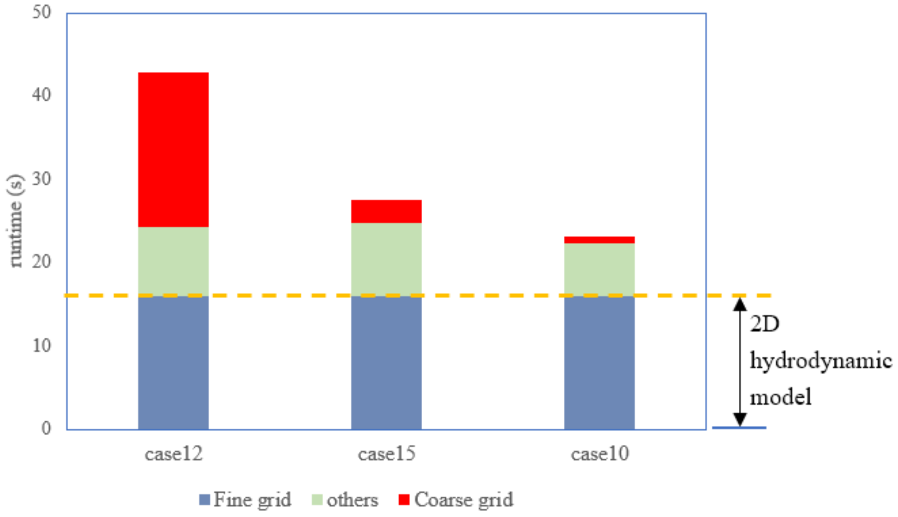

Figure 9 The runtime for coarse and fine grids and the total runtime

Table 2 The number of fine and coarse grids

	Case12	Case15	Case10
The number of fine grids	144	144	144
The number of coarse grids	1400	352	144

There were two reasons to explain the respected reviewer's question. On the one hand, there were large area of fine grid regions, and the number of fine grids was higher than that of coarse grids in all the cases. The 2D hydrodynamic model was solved in the fine-grid regions, which cost more computational time compared with coarse grids. Due to the large amount of calculations involved in fine grids, the time spent on fine grids accounts for a significant proportion of the total execution time. Therefore, the total computational time of all cases does not differ significantly. On the other hand, as the respected reviewer pointed, the 1D hydrodynamic model would be added into the M-DBCM. The 1D hydrodynamic model is used to simulate the flood process in 1D rivers and the 2D hydrodynamic model is only used to simulate the flood process in the low-lying inundation regions. The low-lying inundation regions account for a small proportion of the total watershed regions. Therefore, this will greatly shorten the calculation time.

In future works, we will choose many more appropriate watersheds to evaluate the model performance, where the proportion of low-lying inundation regions to the total watershed area can be further reduced. In addition, the 1D hydrodynamic model will be added to the proposed model.

4. Comment: -l.74 -85 unclear, needs proofreading
Response to comment: We have proofread the manuscript thoroughly, especially the lines from 74 to 85.

5. Comment: -l.117 Ghost cells need to be defined before
Response to comment: We have defined the ghost cells in the introduction.

6. Comment: - l.498 and l.501 "last moment" > in the last time step?
Response to comment: The “last moment” means “in the last time step”. We have revised in the revised manuscript.